RSC Advances

ROYAL SOCIETY OF CHEMISTRY

www.rsc.org/advances

P34HB film promotes cell adhesion, *in vitro* proliferation, and *in vivo* cartilage repair

Na Fu[1#], Jing Xie[1#], Guo Li[1], Xiaoru Shao[1], Sirong Shi[1], Shiyu Lin[1], Shuwen Deng[1], Ke Sun[1], Yunfeng Lin[1*]

[1]*State Key Laboratory of Oral Diseases, West China Hospital of Stomatology, Sichuan University, Chengdu 610041, P. R. CHINA.*

*Corresponding author: Yunfeng Lin,

State Key Laboratory of Oral Diseases, West China Hospital of Stomatology, Sichuan University, Chengdu 610041, P. R. CHINA;

Tel: +86-28-85503487; Fax: +86-28-85582167;

E-mail address: yunfenglin@scu.edu.cn

[#]Na Fu and Jing Xie contribute equally to this work.

The management of chondral defects is a challenging topic of current actuality for scientists and surgeons, resulting in a crucial impact on human costs. For several centuries after its first observation, so far this problem has not found a satisfactory and definitive answer. Cartilage tissue engineering, which involves novel natural scaffolds, has emerged as a promising strategy for cartilage regeneration and repair. In the study, the bio-plasticpoly3-hydroxybutyrate4-hydroxybutyrate (P34HB) film was first fabricated. The characteristics of P34HB film was tested by using SEM and AFM. Cell morphologies on P34HB film were obtained by SEM and fluorescence microscopy after cell seeding. The tests of cell adhesion and proliferation on P34HB film were conducted by the MTT and CCK-8 assay, respectively. Furthermore, the full cartilage defects in rats were created and P34HB films were implanted to evaluate the healing effects within 8 weeks. It was found that P34HB film, as an implant biomaterial, possessed good properties for cell adhesion, migration, and proliferation *in vitro*. Importantly, in *in vivo* experiment, the P34HB film revealed desirable healing outcomes. These results demonstrated that P34HB film was a good scaffold for cartilage tissue engineering through improving the cell proliferation and adhesion.

Introduction

Articular cartilage is frequently damaged due to injury or disease. The damaged cartilage cannot fully regenerate because of its limited intrinsic healing capacity. Furthermore, cartilage injuries always lead to secondary degenerative disease of the involved joint such as osteoarthritis (OA).[1-2] In order to achieve better repair of injured articular cartilage, researchers have optimized clinical methods and proposed various experimental approaches, including abrasion arthroplasty,[3-4] microfracture,[5] and transplantation of chondrocytes,[6-9] perichondrium,[10] meniscal allografts,[11] periosteum,[12] or osteochondral grafts.[13] Additionally, some studies focus on chondrocyte itself. Zhang et al.[14] used the Cre-loxP technique to remove insulin receptor (IR) from chondrocytes and show that the loss of IR signaling causes up-regulation of insulin-like growth factors (IGFs) and insulin-like growth factor (IGF)-1R, which appear to act in a compensatory fashion to regulate the proliferation of chondrocytes. Shen et al.[15] focussed on the function and signaling mechanisms of TGF-β/SMAD pathway which plays a critical role in articular chondrocytes during OA development. However, so far, there is no satisfactory treatment that enables full restoration of injured articular cartilage to its original phenotype. Cartilage tissue engineering has emerged as a promising strategy for cartilage repair that hold the key to the successful regeneration of cartilage tissue.[16] Synthetic and biologically derived materials have been used in tissue engineering and regenerative medicine as an extracellular matrix (ECM) – like fillings which plays a fundamental role in regulating cell attachment, proliferation, migration and differentiation. Some studies show that suitable scaffold material provides high porosity and high surface area for chondrocyte delivery, attachment, growth, and ECM accumulation.[17-19] Currently, further improvements are needed strongly by using desirable scaffold material with better mechanical and biological functions to be grafted to lesion locations to induce *in situ* cell differentiation, proliferation, and chondrogenesis.[20]

Poly (ε-caprolactone) nano-composite scaffolds show the potential in tissue engineering.[21] Natural amorphous co-polymer poly (3-hydroxybutyrate-co-4-hydroxybutyrate) (P34HB), as a member of bacterial biopolyesterpolyhydroxyalkanoate (PHA) family, is becoming a desirable candidate for its remarkable mechanical properties, biocompatibility, and biodegradability.[22-24] It overcomes the brittleness, the narrow processing window of homopolymer poly-3-hydroxybutyrate (PHB),[25] and shows an extension from 45% to 100% to break in accordance with 3~8 mol % 4-hydroxybutyrate.[26] The favorable surface physicochemical properties including hydrophilicity, surface free energy, and polarity determined by high crystallization behavior make it attract great interest as a carrier for long-term release of active biomolecules or for degradable implant materials.[27] Previous *in vivo* studies for application of P34HB in tissue engineering are mainly on the cardiovascular tissues[28-30] and central nervous system[31] but never on cartilage defects.

In our previous study, the results had indicated that P34HB was a good material for tissue engineering.[32-33] Mesenchymal stem cells (MSCs) compose a group of multipotent stem cells derived from adult organs and tissues including bone marrow, ligaments, muscles, adipose tissue, and dental pulp.[34-36] MSCs may undergo self-renewal over several generations while maintaining capacity to differentiate into multi-lineage tissues such as bone, cartilage, muscle and fat.[37] Adipose-derived stem cells (ASCs), as a kind of MSCs, can be readily available, being relatively easily isolated from elective surgery to remove excess adipose tissue. ASCs supplemented with transforming growth factor-beta1 (TGF-β1) can generate proteoglycan rich spheroids that express collagen II, aggrecan, decorin and other markers consistent with chondrogenesis.[38-39] Subcutaneous implantation in immunodeficient mice showed that ASCs can not only retain the chondrocyte phenotype but can also form cartilaginous tissue.[40]

Therefore, in the present study, in order to further mimic the native ECM microenvironment of articular cartilage and improve the biomechanical strength of scaffold microarchitecture, P34HB film were fabricated and characterized. The cell behaviors of ASCs on P34HB film were examined in *vitro*. Importantly, we next surgically created full thickness cartilage defects in rats and implanted P34HB film to evaluate the repair effects within 8 weeks post-surgery. The implantation results based on P34HB film may shed light on its potential in cartilage tissue engineering.

Experimental section

Preparation of P34HB film

The polymer solution was prepared by dissolving 1 g P34HB (molecular weight: 5×10^5, 80% 3HB and 20% 4HB, provided by Tsinghua University, Beijing, China) in 20 mL of organic solvent mixture 4:1 ratio composed of chloroform and dimethylformamide (Sigma, St Louis, MO). The mixed organic solvent was prepared by rotation (60 r/min) overnight.

The P34HB film was obtained by placing the polymer solution in a glass dish (10 cm in diameter and 55 cm^2 in bottom area) and allowing the evaporation of volatile liquid. The thickness of the P34HB film was controlled to be 0.7 mm.

Morphology characterization of P34HB film

Scaffold samples were fixed by 5% glutaraldehyde in 1 × phosphate buffered saline (PBS, pH = 7.4) overnight, dehydrated at the increased concentrations of ethanol (percentage from 30, 50, 70, 90, 95 to 100) and lyophilized (FD-1, Bioking Technology Company, Beijing, China). The samples were then mounted on aluminium stumps, coated with gold in a sputtering device for 1.5 min at 15 mA and examined under a

scanning electron microscope (SEM, HITACHI S-4800, Tokyo, Japan) equipped with EDS (Alpha Ray Spectrometer, Oxford, UK) at an accelerating voltage of 20 kV. The diameter of the P34HB film was measured from the SEM images using image analysis software (Image J, National Institutes of Health, USA) and calculated by selecting 100~150 fibers SEM images randomly.

AFM

The surface roughness of P34HB film was measured by an Atomic Force Microscope (AFM, Nanoscope MultiMode & Explore SPM, Vecco Instrument, US) conducted in ambient air under tapping mode with a scan rate of 0.5 Hz and a scan size of 5 × 5 μm^2. The Root Mean Square (RMS), Surface Area difference and Z range were estimated with the aid of Nanoscope imaging software.

Contact angle measurement

For determination of hydrophilicity of scaffolds, the static contact angle of distilled water on the surface of the P34HB film was measured by a Cam 200 optical contact angle meter (KSV Instruments, Monroe, CT). The images of water drops on the sample surface were recorded by a CCD camera (KGV-5000, Japan), and then analyzed with software supplied by the manufacturer. Six samples were measured in each group. Four different points were measured for each sample. The initially, distilled water (5 μL) was used in each measurement after 3 s exposure at ambient temperature and 65% relative humidity (RH).

Mechanical testing parameters

Mechanical properties of P34HB film were determined by a tabletop uniaxial testing instrument (Instron 5565, USA) using a 50 N load cell under a crosshead speed of 5 mm/min at ambient conditions (RH ~ 65%). All samples were prepared in the form of rectangular shape with dimensions of 10 mm × 60 mm from the P34HB film. The mechanical testing was repeated at least six times. The stress-strain curves, Young's modulus, tensile strength of P34HB film was obtained.

Adipose-derived stem cells (ASCs)

Two-week-old SD rats from the Sichuan University Animal Center and Green fluorescent mice from high techpark of Sichuan University were used in this study, in accordance with International Guiding Principles for Animal Research (1985). Inguinal fat pads were dissected from the mice and were washed extensively in sterile PBS to remove tissue debris. Fat pads were then digested using 0.075% type I collagenase (Sigma-Aldrich, St. Louis, MO, USA) in PBS, for 60 min at 37 °C, with agitation. After neutralization of collagenase, cells released from specimens were filtered and collected by centrifugation at 1200 g for 10 min.

Resulting pellets were resuspended, washed three times in medium and cells were seeded in plastic flasks in control medium (a-MEM, 10% FBS). Cultures were maintained in a humidified atmosphere of 5% CO_2 at t 37 °C and resultant mASCs were passaged three times prior to differentiation or measurement.

Cell morphology

The P34HB film (which were cut into a round shape fitting the well diameter in a 96-well plate and 0.7 mm in thickness) were placed into 96-well plates. All of the materials were irradiated under ultraviolet for half an hour for disinfection. The third passage of rASCs and green fluorescent mASCs were seeded at 5~10 × 10^4/mL density into the glass-bottomed 96-well plates which was prepared as described above. For SEM, after cell seeding for 1, 3, 5, and 7 days, cells attached and infiltrated into P34HB film were fixed with 3% glutaraldehyde for 1 h, rinsed three times in water and dehydrated with graded concentrations of ethanol (percentage from 50, 70, 90, to 100, v/v). Subsequently the samples were treated with hexamethyldisiloxane (HMDS) and kept in a fume hood for air drying. Finally the samples were coated with gold for the observation of cell morphologies.

The third passage of green fluorescent mASCs were seeded at 5~10 × 10^4/mL density into the glass-bottomed 6-well plates which was prepared as described above. For comparison purposes, the control group which the green fluorescent mASCs were seeded at 5~10 × 10^4/mL density into the 6-well plates without scaffold materials was established. For each group, two paralleled holes were set up. After 1 day, 5 days and 7 days of cell culturing in the basic medium, they were taken using an Olympus IX 710 microscope (Olympus, Tokyo, Japan).

Cell adhesion assay

The P34HB film (which were cut into a round shape: like a hole of 96-well plate in diameter and 0.7 mm in thickness) were placed into 96-well plates for half an hour under ultraviolet disinfection. The third passage of rASC were seeded at 10^5/mL density into flasks, and on glass coverslips into the 96-well plates which have been putted in P34HB film at an appropriate initial density. The control group was established in which the rASCs was seeded at 10^5/mL density into the 96-well plates without scaffold materials. For each group, three paralleled holes were set up. After 2 hours, 4 hours, 8 hours of cell culturing in the basic medium, a 3-(4,5-dimethylthiazol-2-yl)-2,5-diphenyl-tetrazolium bromide (MTT) assay was carried out to quantify the amount of viable cells to determine the extent of cell adhesion on the P34HB film. The MTT assay is based on the reduction of the yellow tetrazolium salt to purple formazan crystals by dehydrogenase enzymes secreted from the mitochondria of metabolically active cells. The amount of purple formazan crystals formed is proportional to the number of viable cells. First, each culture medium was aspirated and replaced

with 200 μL per well of MTT solution at 0.1mg mL-1 for a 96-well culture plate. Secondly, the plate was incubated for 4 h at 37 °C. The solution was then aspirated and 150 μL per well of dimethylsulfoxide (DMSO) was added to dissolve the formazan crystals. Finally, after 10 min of rotary agitation, the absorbance of the DMSO solution at 570 nm was measured by using a Thermospectronic Genesis10 UV/Visible spectrophotometer (Thermo Electron Corp, USA).

Cell proliferation assay

For cell proliferation, the cell counting assay kit-8 (CCK-8) (Dojindo, Japan) was used to quantify the amount of viable cells to determine the extent of cell proliferation and cytotoxicity on the P34HB film after cell at 10^5/mL density seeding for 1, 3, 5, and 7 days. Briefly, 10 μL of CCK-8 solution was added to each well of a ninety six-well plate with or without scaffolds. The loaded samples were incubated at 37 °C for 1 ~ 4 h to form the water dissoluble formazan. The optical density (OD) value was measured at a wavelength of 450 nm by micro-plate reader (VariOskan Flash 3001, Thermo, USA). The amount of the formazan dye, generated by the activity of dehydrogenases in cells was directly proportional to the number of living cells. The samples included the normal control group and P34HB film groups; all treated groups were normalized to the control group.

In *vivo* cartilage defect formation

Thirty 12-week-old SD rats (30) were used in this study. The animals were anesthetized with chloral hydrat by intraperitoneal injection. A medial parapatellar skin incision was made, and the knee joint was exposed via lateral dislocation of the patella. Full thickness cartilage defects that extend through the cartilage layer and penetrate the subchondral bone were created surgically at the femoropatellar groove of both hind leg knee joints. The defects were made at 1.5 mm in diameter and 2 mm in depth as previously described.[41]

***In vivo* implantation**

The P34HB film (which were cut into a round shape: l.5 mm in diameter and 0.7 mm in thickness) were placed into 96-well plates for half an hour under ultraviolet disinfection).

12-week-old (30) SD rats were used to generate 60 defect samples (bare P3HB4HB scaffolds: 40 samples; and chondrocyte defects without treatment: 20 samples (controls). Immediately after formation of cartilage defect in rats, the implantation was carried out by filling the overlapped scaffolds into the defect holes. Rats were sacrificed after 4 (10 rats, 20 samples) and 8 (10 rats, 20 samples) weeks to assess the repair process of cartilage effects, respectively. The defects were made at 1.5 mm in diameter and 2 mm in depth, so, we used the 1.5mm diameter and 0.7 mm thickness film to fill the defects, Specific methods used, are as follows: we

first put a layer of P34HB film on the defect through extrusion as this could make the P34HB film stable in the defect region, and so on, until the defect area was filled.

Histological staining and immunohistochemistry

For histological evaluation, implantation sites were harvested and fixed in 4% PFA for 48 h at 4℃. Samples were dried through a series of graded alcohol baths for dehydration and in xylene, embedded in paraffin and sectioned into slices with a 5 μm - thickness. Sections were stained with hematoxylin and eosin (HE, Beyotime, China), Alcian blue and Safranin O staining (Sigma-Aldrich, USA).

For immunohistochemistry, the slices were stained with rat polyclonal antibodies against rat type II collagen (No.bs-0709R, Bioss, Beijing, China) and goat anti-rat IgG/biotin (No.SP-0023, Bioss, Beijing, China) according to a standard SABC protocol according to the manufacturer. The rehydrated paraffin sections were treated with 0.1% trypsin for epitope unmasking before staining. Three samples for each group were analyzed by an inverted light microscopy (Olympus-IX71, Japan).

Statistical analysis

Results are expressed as means ± standard deviations. Statistical analysis was performed by using Student's *t*-test as well as one-way analysis of variance (ANOVA) followed by SPSS 19.0 software (SPSS, USA). In each analysis, the critical significance level was set at $p < 0.05$.

Results

Characteristics of P34HB film

The morphologies of P34HB film were firstly characterized by AFM (Fig.1a). To show a representative topological morphology, we chose a random size at 10 × 10 μm. The quantified surface roughness was about 578.19 nm in height. As the P34HB film featured a high specific surface area, one of the decisive factors for micro-scale materials was wettability, the contact angle was determined at 96.1° to 60.15°C by a Cam 200 optical contact angle meter instrument (Fig. 1b). In the tension test, the P34HB film could bear the tensile force up to 8 N, and the tensile displacement was reached to ~ 15 mm before its fragmentation (Fig. 1c). At the scaffold size of 10 × 5 × 0.7 mm, the mechanical parameters were measured (Fig.1d). The Young's modulus were about 13.9291 MPa, Tensile strength approximately up to 1.2324 MPa.

Cell behaviors of ASCs in response to P34HB film in *vitro*

The morphologies of P34HB film were next characterized by SEM at different size (400-50 μm, HV: 20.00 kv, mode: SE) (Fig.2a). The ASCs isolated from rats were seeded onto the P34HB film and the rASCs were

attached to the P34HB film 8 h after seeding. The attached rASCs were showed in Fig.2a by SEM. At 3 day after seeding, the cell spreading area was broadest. Then, the number of rASCs was significantly increased and up to confluence at 7 day.

We further used ASCs from green fluorescent mice to obtain the cell morphology seeded onto the P34HB film (Fig. 2b). The results were consistent with Fig.2a by SEM. In petri dish control group, the mASCs were seeded, attached, spread, and proliferated within 7 days. For P34HB film, the cell spreading area of mASCs was also broadest the same as Fig.2a by SEM, and the numbers were increasing compared with control group.

A cell adhesion assay was carried out indirectly by quantifying the amount of trypsinised cells adhered onto the scaffolds at 2, 4, and 8 h post-seeding. The MTT showed After 2, 4 and 8 h culture, cells on P34HB film exhibited much greater average absorbance values in compared to controls (Fig. 2c). The proliferation assay was then performed to evaluate the cell proliferation rate on the scaffolds by CCK-8 kit (Fig.2d). The results showed that, after 3 day, the rASCs on the P34HB film had a significantly higher proliferation rate than on the petri dish group (up to ~ 81 %)

Knee cartilage defect and biomaterial implantation: P34HB film in cartilage tissue engineering

P34HB based on PHA polymers could fill the site of cartilage defect for its good mechanical properties and biocompatibility (Fig.1 and 2). During *in vivo* experiments, full thickness cartilage defects at hind knee were carried out by using 12-week-old SD rats. The sites of defects were surgically created at the femoropatellar groove (1.5 mm in diameter, 2 mm in depth). The groups were divided into two sub-groups including P34HB film implant group (20 rats, 40 samples) and bare chondrocyte defect group without any treatment (10rat, 20 samples). The wounds were sutured immediately after scaffold materials implanted. Animals post-surgery maintained in good health throughout the study, as assessed by their weight gain. Experimental rats were sacrificed and the repairs of cartilage defect were detected at 4 and 8 week post-surgery (Fig.3). At 4 week, the new-formed tissues could not cover the defects in all groups. At 8 week, the implantation groups had formed repaired morphologies of cartilage defect. The control group showed the reduced defect area but did not form repair morphology and the P34HB film implant indentation of cartilage defects showed integral repair morphology but the embedded P34HB film did not show to be degradation.

Repair evaluation: from histological staining to immunohistochemistry

The samples from the repair sites of cartilage defects at 4 and 8 week post-surgery were evaluated by HE, Toluidine Blue O, Alcian blue and type-II collagen stains (Fig. 4 and 5).

HE stain showed the interface between peri-native tissues and new-formed tissues in all groups. The

control group (8week) showed the reduced defect area but did not form repair morphology. Among the implant groups, the interfaces at 4 week were more distinct compared with those at 8 week post-surgery. At 4 week, the layers of P34HB film were clearly shown, but the newly formed tissue (NT, Fig.4 the second vertical column at 4 week) was gradually covered at the top of cartilage defect indentation. At this time, the original tissue (OT), newly formed tissue (NT), and P34HB film (F) were all clearly observed at the site of cartilage defects. At 8 week, a better repaired new-formed tissue gradually covered the P34HB film to form integral cartilage-like tissue. From toluidine blue O stain, we further confirmed that, at 8 week post-surgery, the newly formed tissue were shown to be integral and cartilage-like although, at 4 week, OT, NT, and F were all clearly observed at the site of cartilage defects (Fig.4).

We further evaluated the components of proteoglycan and collagen II at the repair sites by using alcian blue and type II collagen stain (Fig.5). From the alcian blue stain, we found that, the control group (8week) showed the reduced defect area but did not form repair morphology. Among the implant groups, at 4 week post-surgery, there were distinctly differences between original tissue and newly formed tissue. The newly formed tissue showed light colour in relative to the original tissue, although the newly formed tissue showed the component of proteoglycan. At 8 week, the newly formed tissue were completely covered the implant material and formed an integral surface at ~ 400 μm in thickness. But the P34HB films were embedded in the deep defects and did not degrade. Type II collagen is another important marker to evaluate the cartilage repair. The interfaces between peri-native tissue and new-formed tissue were distinct at 4 weeks. At the top of the indentation of cartilage defects, there had formed a thin layer of Type II collagen – contained new tissue, and this newly formed tissue did not form an integral surface. At 8 week, the original tissue and newly formed tissue were fused and an integral surface formed.

Discussion

Biomimetic scaffolds using natural and synthetic biomaterials are highly desireable to recreate the micro-architecture of articular cartilage. Although intensive researches have been focused on the developmental biology and regeneration of cartilage tissue and a diverse plethora of biomaterials has been developed for this purpose, cartilage regeneration is still suboptimal, such as lacking a layered structure, mechanical mismatch with native cartilage and inadequate integration between native tissue and implanted scaffold.[42-43]After characterizing P34HB film, we found it suitable for implantation for cartilage defect as a relatively favorable natural biomaterial, especially for its intrinsic hydrophily.

P34HB has been shown to have a wide range of physical properties ranging from high crystalline to elastic character depending on mol (%) of 4HB monomer. [23,27,38,44] Crystallization plays an important role in

changing hydrophilicity, surface free energy, and polarity, [26,39] thus affects cell attachment and proliferation. [45] For the experiments *in vitro*, the crystallization at 45% was found to support RaSMCs cell growth the strongest in corresponds to a 7% 4HB in P3HB4HB.[26] In addition, material surface morphology also decides the cell viability and growth behaviors.[40,46] RaSMCs grew well in all P3HB4HB scaffolds, and on P (3HB-7% 4HB) films and scaffolds, the cells proliferated the best.[26] In our study, we found the cell adhesion and proliferation were high in relative to petri dish control group due to the good physical properties of P34HB film. The *in vitro* cell experiments provide a direct support for the next implant study.

A successful implant biomaterial should meet an important requirement - the controllable degradation of the implant and the followed integration between native tissues and films (scaffolds). The degradation products of P34HB film based on PHAs were Oligo-HAs, including oligo (3-hydroxybutyrate) (OHB) and oligo (3-hydroxybutyrate-co-3-hydroxyhexanoate) (OHBHHx). Previous studies on murine beta cells had directly confirmed these degradation products had positive effects on cell growth.[47] *In vitro*, the ability of promoted proliferation on P34HB film after one week's culture also indirectly reflected the positive ability of cell growth (Fig.2). In implantation based on P34HB film, the surface morphology showed a formed a layer of cartilage tissue that resembled native cartilage (Fig.3 and 4). The degradation rate of P34HB film might perfectly match the growth of new cartilage.

There are still some limitations in the current study. Firstly, whether the new repaired tissue is the cartilaginous tissue or fibro-cartilaginous tissue needs a long-term follow up to be further investigated, although the morphology, histological staining and immunohistochemistry have confirmed the markers of cartilages in new-formed tissues. Secondly, the time during which P34HB film could entirely degrade and the new cartilage could be completely formed, should be confirmed. Thirdly, whether the mechanical properties of newly formed tissues are closed to those of native cartilage also needs to be further investigated.

Conclusions

In this study, the P34HB film was fabricated and its the mechanical properties were determined. The adipose-derived stem cells (ASCs) were seeded onto the films to evaluate their abilities of adhesion, and proliferation. It was established that cells seeded onto the films had better abilities of adhesion and proliferation *in vitro*. Furthermore, the actual thickness cartilage defects were created at the site of the femoropatellar groove of rat knee and the P34HB film scaffold were immediately implanted. After 8 weeks post-surgery, new cartilage-like tissues were formed at the sites of defects. By evaluation from histological staining to immunohistochemistry, a better integration between native tissues and scaffolds were confirmed.

Our findings demonstrated that P34HB film scaffold had exhibited a great potential in the field of tissue engineering and could lead to excellant repair of cartilage defect.

Acknowledgments

This work was funded by National Natural Science Foundation of China (81470721, 31170929), Sichuan Science and Technology Innovation Team (2014TD0001), and Funding of State Key Laboratory of Oral Diseases (SKLOD201405).

References

1. D. W. Jackson and T. M. Simon, *Arthroscopy ,* 1996, **12**, 732-738.
2. A. P. Newman, *Am. J. Sports. Med.,* 1998, **26**, 309-324.
3. J. M. Bert, Rheum. *Dis. Clin. North. Am.,* 1993, **19**, 725-739.
4. L. L. Johnson, *Arthroscopy,* 1986, **2**, 54-69.
5. T. Minas and S. Nehrer, *Orthopedics*, 1997, **20**, 525-538.
6. M. Brittberg, A. Lindahl, A. Nilsson, C. Ohlsson, O. Isaksson and L. Peterson, *N. Eng. J. Med.*, 1994, **331**, 889-895.
7. D. A. Grande, M. I. Pitman, L. Peterson, D. Menche and M. Klein, *J. Orthop. Res.*, 1989, **7**, 208-218.
8. K. Katsube, M. Ochi, Y. Uchio, S. Maniwa, M. Matsusaki, M. Tobita and J. Iwasa, *Arch. Orthop. Trauma. Surg.*, 2000, **120**, 121-127.
9. S. Shortkroff, L. Barone, H. P. Hsu, C. Wrenn, T. Gagne, T. Chi, H. Breinan, T. Minas, C. B. Sledge, R. Tubo and M. Spector, *Biomaterials*, 1996, **17**, 147-154.
10. D. Amiel, R. D. Coutts, M. Abel, W. Stewart, F. Harwood and W. H. Akeson, *J. Bone. Joint. Surg. Am.*, 1985, **67**, 911-920.
11. Y. Sumen, M. Ochi and Y. Ikuta, *Arthroscopy,* 1995, **11**, 185-193.
12. V. E. Hoikka, H. J. Jaroma and V. A. Ritsila, *Acta. Orthop. Scand.*, 1990, **61**, 36-39.
13. Y. Matsusue, T. Yamamuro and H. Hama, *Arthroscopy*, 1993, **9**, 318-321.
14. F. Zhang, Q. He, W. P. Tsang, W. T. Garvey, W. Y. Chan and C. Wan, *Bone Research*, 2014, **2**.
15. J. Shen, S. Li and D. Chen, *Bone Research*, 2014, **2**.
16. K. Ye, R. Felimban, S. E. Moulton, G. G. Wallace, C. Di Bella, K. Traianedes, P. F. Choong and D. E. Myers, *Regen. Med*, 2013, **8**, 333-349.
17. J. Xu, S. Li, F. Hu, C. Zhu, Y. Zhang, W. Zhao, T. Akaike and J. Yang, *J. Nano. Nanotechno.*, 2014, **14**, 4007-4013.
18. N. Ma, C. Ma, C. Li, T. Wang, Y. Tang, H. Wang, X. Moul, Z. Chen and N. Hel, *J. Nanosci. Nanotechnol.*, 2013, **13**, 6485-6498.
19. G. Amsaveni, A. S. Farook, V. Haribabu, R. Murugesan and A. Girigoswami, *Adv. Sci. Eng. Med.* , 2013, **5**, 1340-1348.
20. W. Zhao, X. Jin, Y. Cong, Y. Liu and J. Fu, *J. Chem. Technol. Blot.*, 2013, **88**, 327-339.
21. V. J. Mkhabela and S. S. Ray, *J. Nanosci. Nanotechnol.*, 2014, **14**, 535-545.
22. R. Luo, K. Xu and G. Q. Chen, *J. Appl. Polym. Sci.*, 2007, **105**, 3402-3408.
23. L. Luo, X. Wei and G.-Q. Chen, *J. Biomater. Sci. Polym. Ed.,* 2009, **20**, 1537-1553.
24. C.-L. Dong, S.-Y. Li, Y. Wang, Y. Dong, J. Z. Tang, J.-C. Chen and G.-Q. Chen, *Biomaterials*, 2012, **33**, 2593-2599.
25. X.-T. Li, Y. Zhang and G.-Q. Chen, *Biomaterials*, 2008, **29**, 3720-3728.
26. S.-T. Cheng, Z.-F. Chen and G.-Q. Chen, *Biomaterials*, 2008, **29**, 4187-4194.
27. X.-D. Yang, X.-H. Zou, Z.-W. Dai, R.-C. Luo, C.-J. Wei and G.-Q. Chen, *J. Biomater. Sci. Polym. Ed.*, 2009, **20**, 1729-1746.
28. R. Sodian, S. P. Hoerstrup, J. S. Sperling, S. H. Daebritz, D. P. Martin, F. J. Schoen, J. P. Vacanti and J. E. Mayer Jr, *Ann.*

Thorac. Surg. , 2000, **70**, 140-144.

29. F. Opitz, K. Schenke-Layland, T. U. Cohnert, B. Starcher, K. J. Halbhuber, D. P. Martin and U. A. Stock, *Cardiovasc. Res.*, 2004, **63**, 719-730.
30. U. A. Stock, T. Sakamoto, S. Hatsuoka, D. P. Martin, M. Nagashima, A. M. Moran, M. A. Moses, P. N. Khalil, F. J. Schoen and J. P. Vacanti, *J. Thorac. Cardiovasc. Surg.*, 2000, **120**, 1158-1167.
31. X.-Y. Xu, X.-T. Li, S.-W. Peng, J.-F. Xiao, C. Liu, G. Fang, K. C. Chen and G.-Q. Chen, *Biomaterials*, 2010, **31**, 3967-3975.
32. N. Fu, S. Deng, Y. Fu, G. Li, X. Cun, L. Hao, X. Wei, X. Cai, Q. Peng and Y. Lin, *Cell Prolif.*, 2014, **47**, 465-475.
33. G. Li, N. Fu, J. Xie, Y. Fu, S. Deng, X. Cun, X. Wei, Q. Peng, X. Cai and Y. Lin, *J. Biomed. Nanotechnol.*, 2015, **11**, 105-116.
34. A. Vats, N. Tolley, J. Polak and L. Buttery, *Clin. Otolaryngol. Alli. Sci.*, 2002, **27**, 227-232.
35. K. Turksen, *Dev. cell.*, 2004, **6**, 454-456.
36. B. E. Grottkau, P. P. Purudappa and Y.-f. Lin, *Int. J. Oral. Sci.*, 2010, **2**, 21.
37. K. Le Blanc and M. Pittenger, *Cytotherapy*, 2005, **7**, 36-45.
38. B. Levi and M. T. Longaker, *Stem Cells*, 2011, **29**, 576-582.
39. H. Mizuno, M. Tobita and A. C. Uysal, *Stem Cells*, 2012, **30**, 804-810.
40. G. R. Erickson, J. M. Gimble, D. M. Franklin, H. E. Rice, H. Awad and F. Guilak, *Biochem. Biophys. Res. Commun.*, 2002, **290**, 763-769.
41. R. Kuroda, A. Usas, S. Kubo, K. Corsi, H. Peng, T. Rose, J. Cummins, F. H. Fu and J. Huard, *Arthritis Rheumatism*, 2006, **54**, 433-442.
42. Y. Zhu, M. Yuan, H. Meng, A. Wang, Q. Guo, Y. Wang and J. Peng, *Osteoarth. Cartilage.*, 2013, **21**, 1627-1637.
43. G. Filardo, H. Madry, M. Jelic, A. Roffi, M. Cucchiarini and E. Kon, *Knee. Surg, Sport.Tr, A.,* 2013, **21**, 1717-1729.
44. M. Gomez‐Camarillo, M. Almonte‐Becerril, M. Vasquez Tort, J. Tapia‐Ramirez and J. Kouri Flores, *Cell Prolif.*, 2009, **42**, 207-218.
45. L. Wu, H.-J. Prins, M. N. Helder, C. A. van Blitterswijk and M. Karperien, *Tissue. Eng. Part A.*, 2012, **18**, 1542-1551.
46. R. Huang, H. Deng, T. Cai, Y. Zhan, X. Wang, X. Chen, A. Ji and X. Li, *J. Biomed. Nanotechnol.*, 2014, **10**, 1346-1358.
47. J. Sun, Z. Dai, Y. Zhao and G.-Q. Chen, *Biomaterials*, 2007, **28**, 3896-3903.

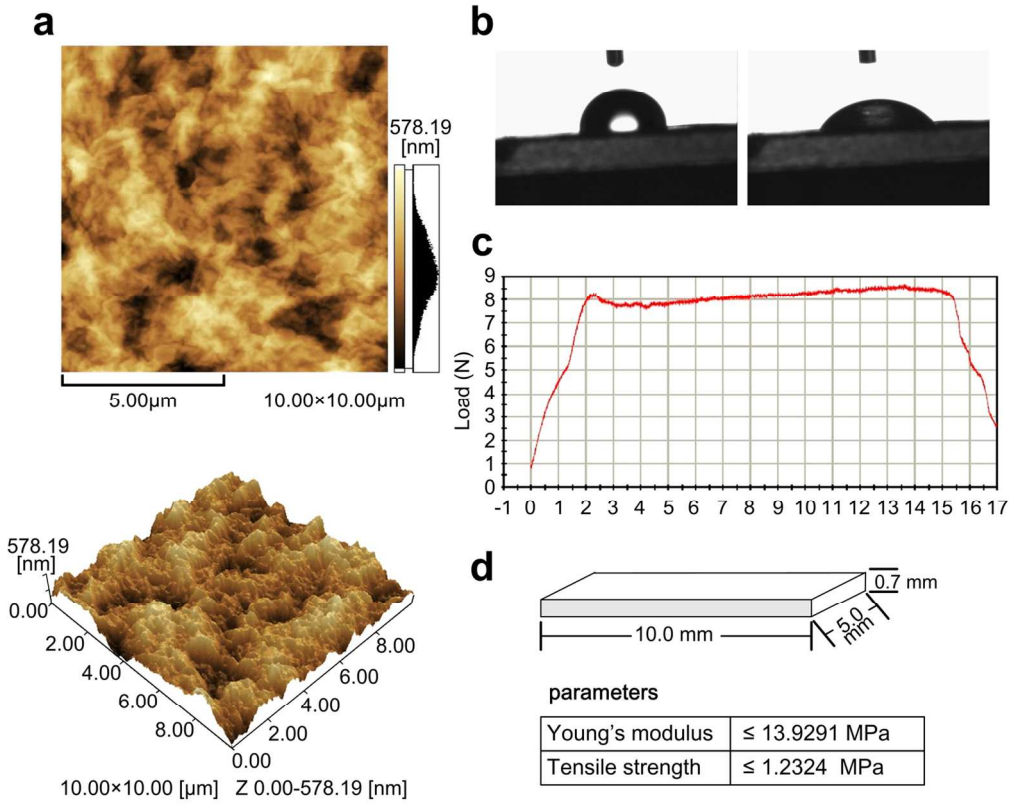

Characterization of P34HB film.
a. Morphology of the P34HB film evaluated by AFM (n = 3). The topological structure of P34HB film was detected randomly at 10 × 10 μm. The quantified surface roughness was 578.19 nm in height.
b. Measurement of water contact angle - wetting behavior of a water droplet on P34HB film (n = 3). Furthermore, the contact angle was determined at 96.1° to 60.15°C.
c. Representative tensile force test curve using tabletop uniaxial testing method (n = 6). The P34HB film could withstand tensile force of up to 8N, and the tensile displacement reached ~ 15m before failure.
d. Mechanical parameters determined from slices of the P34HB film (10.0 × 5.0 × 0.7m) (n = 3). The Young's modulus was approximately up to 13.9291 MPa, the tensile strength was up to 1.2324 MPa.

140x114mm (300 x 300 DPI)

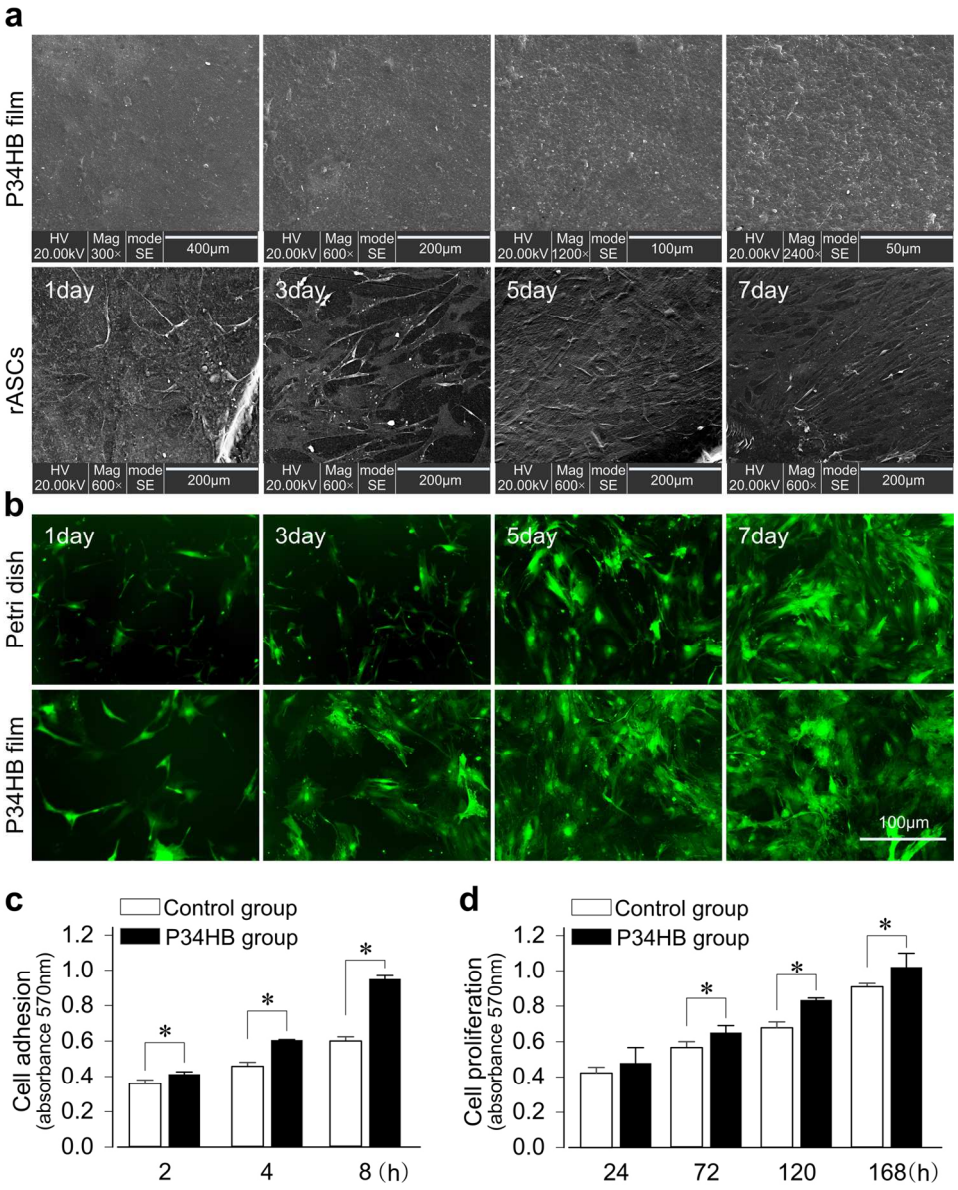

In vitro cell behaviors on the P34HB film.

a. The topological morphologies of the P34HB film at different sizes (the upper row) and cell morphologies of ASCs on P34HB film at different days (the lower row) as shown by SEM (n = 3).

b. Cell morphologies of ASCs from green fluorescent mice seeded on the P34HB film at different days. The Petri dish group showed the normal morphologies of cultured ASCs at different days. The P34HB film group showed the morphologies of cultured ASCs on P34HB film at different days. (n = 3).

c. Cell adhesion of ASCs on P34HB film and petri dishes (n = 3). The adhesion of ASCs on the P34HB films was significantly higher than on the petri dishes.

d. Cell proliferation of ASCs on P34HB film and petri dishes (n = 3). The results showed that the proliferation rates within 7 days were significantly higher on the films than on the petri dishes.

140x176mm (300 x 300 DPI)

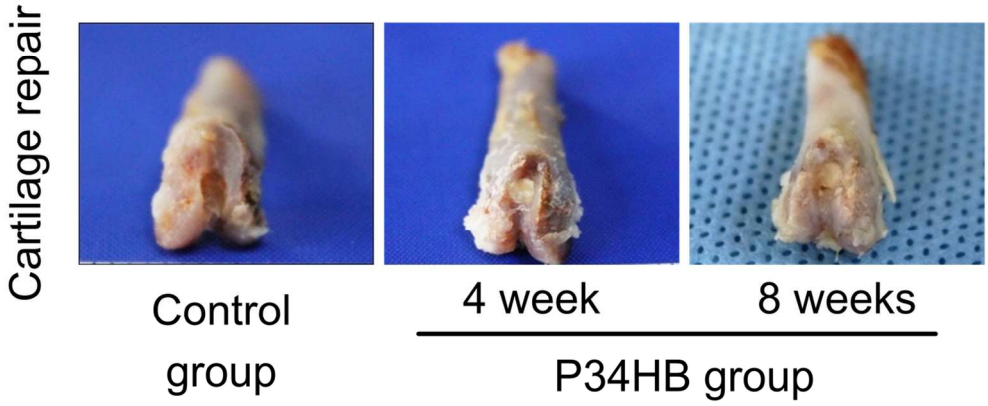

The morphologies of cartilage defects.
The control group (8 week) showed the reduced defect area but did not form repair morphology. While by the P34HB group, at 4 week, we can see the new-formed tissues could not cover the defects in all groups, and at 8 week, the implantation groups had formed repaired morphologies of cartilage defect.

60x26mm (600 x 600 DPI)

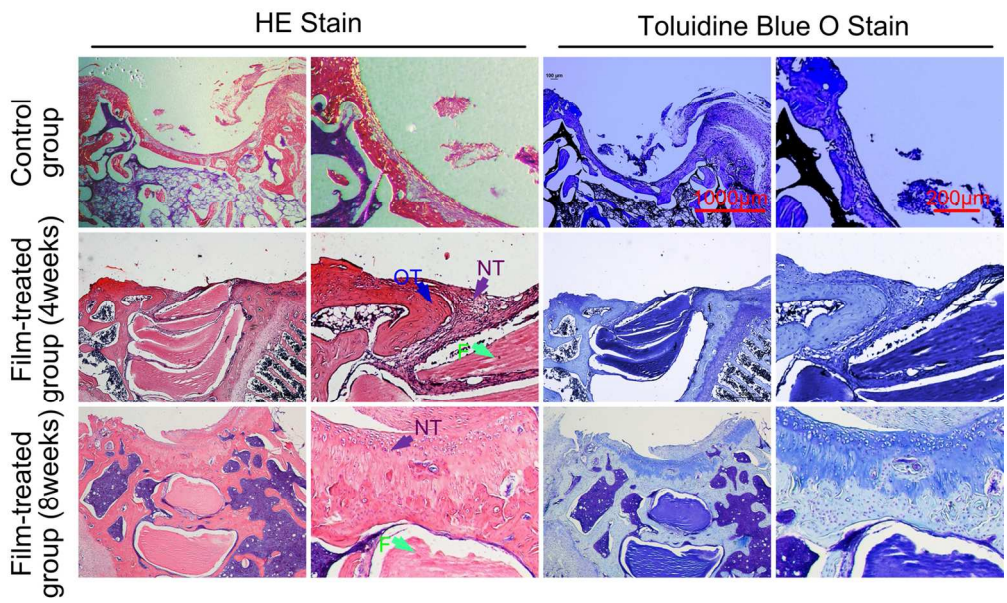

HE and toluidine Blue O staining of cross-sections of repaired knee articular cartilage at 4 and 8 weeks. The control group (8week) showed the reduced defect area but did not form repair morphology. Among the implant groups, the interfaces were more distinct at 4 weeks than at 8 weeks post-surgery. At 8 weeks, reparative newly formed tissue gradually covered the implanted films to form integral cartilage-like tissue. OT = Original Tissues; NT = Newly Formed Tissues; F = implanted P34HB films. The experiments were repeated at 3 times (n = 3).

140x83mm (300 x 300 DPI)

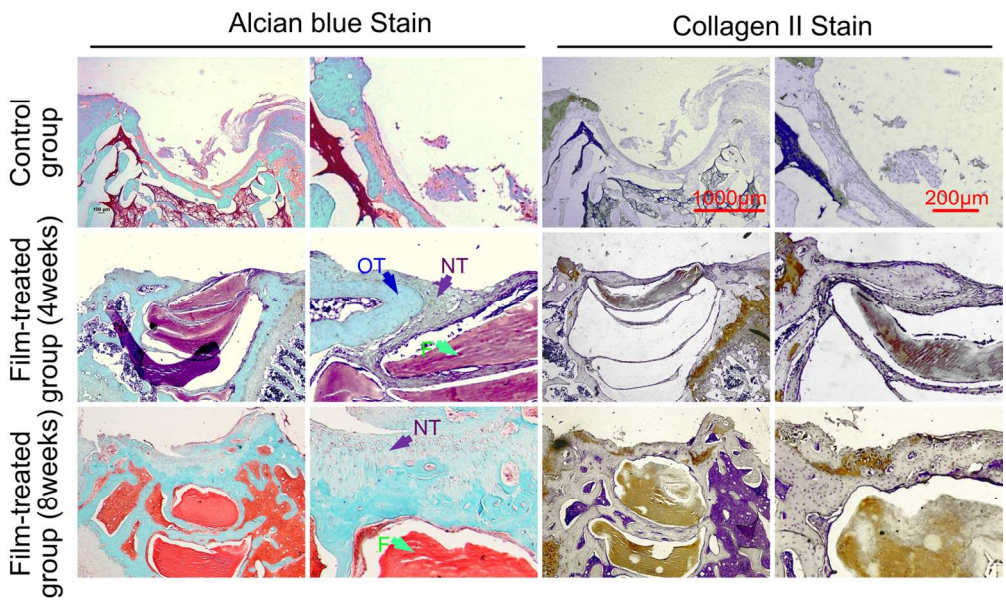

Alcian blue and type-II collagen staining of cross-sections of repaired knee articular cartilage at 4 and 8 weeks.
The control group (8week) showed the reduced defect area but did not form repair morphology. The interfaces between peri-native and newly formed tissue were distinct at 4 weeks after P34HB film implantation. At 8 weeks, the newly formed tissue was covered the implanted films to form integral cartilage-like tissue. OT = Original Tissues; NT = Newly Formed Tissues; F = implanted P34HB films. The experiments were repeated at 3 times (n = 3).

140x83mm (300 x 300 DPI)